Cellular and Molecular Neurobiology (2019) 39:637–650
https://doi.org/10.1007/s10571-019-00668-6

ORIGINAL RESEARCH

Involvement of RhoA/ROCK Signaling in Aβ-Induced Chemotaxis, Cytotoxicity and Inflammatory Response of Microglial BV2 Cells

Xiaoxu Zhang[1] · Piao Ye[1] · Dandan Wang[1] · Yunsheng Liu[1] · Lan Cao[1] · Yancong Wang[1] · Yuxia Xu[1] · Cuiqing Zhu[1]

Received: 7 November 2018 / Accepted: 28 February 2019 / Published online: 9 March 2019

Abstract

Reactive microglia clustering around amyloid plaques in brain is a histopathological feature of Alzheimer's disease (AD) and reflects the contribution of neuroinflammation in AD pathogenesis. β-Amyloid peptide (Aβ) has been shown to induce a range of microglial responses including chemotaxis, cytotoxicity and inflammation, but the underlying mechanism is poorly understood. Considering the fundamental role of RhoA/ROCK signaling in cell migration and its broad implication in AD and neuroinflammation, we hypothesized that RhoA/ROCK signaling might be involved in Aβ-induced microglial responses. From in vivo mouse models including APP/PS1 transgene and fibrillar Aβ stereotactic injection, we observed the elevated expression level of RhoA in reactive microglia. Through a series in vitro cell migration, cytotoxicity and biochemistry assays, we found that RhoA/ROCK signaling plays an essential role in Aβ-induced responses of microglial BV2 cells. Small molecular agents Fasudil and Y27632 showed prominent beneficial effects, which implies the therapeutic potential of RhoA/ROCK signaling inhibitors in AD treatment.

Keywords Aβ · Microglial BV2 cells · RhoA/ROCK signaling · Chemotactic migration · Cytotoxicity · Inflammatory response

Introduction

Alzheimer's disease (AD) is one of the most common chronic neurodegenerative diseases in the aging population (Sindi et al. 2015). The neuropathological hallmarks of AD are extracellular amyloid plaques, intracellular neurofibrillary tangles and extensive neuronal loss (Holtzman et al. 2011). Although increasing numbers of risk factors involved in AD pathogenesis have been discovered, β-amyloid (Aβ) peptide, the main component of amyloid plaques, has been widely accepted as the primary factor. The production and deposition of Aβ severely impair neuronal functions and initiates a variety of pathological changes, including neuroinflammation (Selkoe and Hardy 2016).

Microglia are the major innate immune cells in brain, which respond to pathological conditions and mediate inflammatory response in its reactive states (Wolf et al. 2017). Previous

Electronic supplementary material The online version of this article (https://doi.org/10.1007/s10571-019-00668-6) contains supplementary material, which is available to authorized users.

✉ Yuxia Xu
xuyuxia@fudan.edu.cn

✉ Cuiqing Zhu
cqzhu@shmu.edu.cn

Xiaoxu Zhang
15211010014@fudan.edu.cn

Piao Ye
17211010012@fudan.edu.cn

Dandan Wang
12111010051@fudan.edu.cn

Yunsheng Liu
15111010012@fudan.edu.cn

Lan Cao
13111010004@fudan.edu.cn

Yancong Wang
16111010022@fudan.edu.cn

[1] Department of Translational Neuroscience, Jing'an District Centre Hospital of Shanghai, State Key Laboratory of Medical Neurobiology & Institutes of Brain Science, Fudan University, 138 Yi-Xue-Yuan Road, Shanghai 200032, China

studies based on AD mouse models and human patients have commonly described the phenomenon of reactive microglial clustering around amyloid plaques (Sheng et al. 1997; Solito and Sastre 2012; Meraz-Rios et al. 2013). The accumulation of reactive microglia is not simply due to the proliferation of residential microglia (Venneti et al. 2009), but also a consequence of reactive microglia migration (Villegas-Llerena et al. 2016). Principally, reactive microglia utilize the chemotactic response to sense the pathogens and migrate to spatial targeting locations. It is a chemoattractant-dependent process which requires the integration and coordination of specific cell surface receptor and intracellular signaling (Fan et al. 2017). In the scenario of AD, Aβ has been identified as a direct chemoattractant for microglia chemotaxis, much less is known about the underlying mechanism, especially the intracellular signaling.

Rho subfamily GTPases member RhoA and its downstream effector Rho-dependent coiled-coil kinase (ROCK) have pleiotropic functions in regulating cellular polarity, adhesion, contraction and migration (Raftopoulou and Hall 2004). The involvement of RhoA/ROCK signaling in AD pathology has been documented, such as aluminum-induced amyloid fibril formation in cultured rat cortical neurons (Chen et al. 2010), Aβ-induced neurite retraction (Tsushima et al. 2015), blood–brain barrier disruption (Park et al. 2017) and synaptotoxicity (Sellers et al. 2018). In addition, RhoA/ROCK signaling is also engaged in modulating microglial functions, including both phagocytosis (Scheiblich and Bicker 2017) and neuroinflammation (Alokam et al. 2015; Chen et al. 2017b). Moreover, pioneer studies have reported that RhoA/ROCK signaling participates in the interaction of Aβ and microglia (Jeon et al. 2008; Moon et al. 2013). Thus, considering these broad implications of RhoA/ROCK signaling in cell migration, Aβ toxicity and microglial response, we speculate that RhoA/ROCK signaling might serve as the intrinsic mediator of Aβ-induced microglial chemotaxis, cytotoxicity and inflammatory response.

In this study, we conducted a series in vitro experiments and combined with in vivo models to test this hypothesis. We found that RhoA/ROCK signaling is essential for Aβ-induced responses in microglial BV2 cells including chemotactic migration, cytotoxicity and inflammatory response. Inhibition of RhoA/ROCK signaling can significantly ameliorate these responses, which provides evidence to support the therapeutic potential of RhoA/ROCK inhibitor in AD.

Materials and Methods

Animals

Adult wild-type C57BL/6J mice were purchased from Shanghai Experimental Animal Center of Chinese Academy of Sciences. APPswe/PS1ΔE9 (APP/PS1) transgenic mice were obtained from Shanghai Research Center for Model Organism. All animals were housed in a 12-h light/dark cycle with food and water ad libitum and performed in accordance with the guide for Shanghai Medical Laboratory Animal Care and Use Committee.

Materials

Primary antibodies and reagents are as follows: RhoA, ROCK2, Iba-1 and CD16 (Abcam, USA), CD206 (R&D, USA), β-actin (Santa Cruz, USA), NLRP3, Caspase1 and IL-1β (ABclonal, China), Rho Activation Assay Kit (Millipore, USA), 3-Well Chamber Insert (Ibidi, USA), Falcon Cell Culture Insert (Transwell) (Corning Brand, USA), ActinOrange™ 555 Stain (GeneCopoeia, USA), $A\beta_{1\text{-}42}$ peptide (ChinaPeptides, China), poly-D-lysine (PDL; Sigma-Aldrich, USA), Cell Counting Kit-8 (CCK-8, Dojindo, Japan), Cytotoxicity Detection Kit^{PLUS} (LDH, Roche, USA), Fasudil and Y27632 (Selleck, USA), lipopolysaccharide (LPS, Sigma-Aldrich, USA), IL-1β ELISA kit (ABclonal, China).

Preparation of Fibrillar $A\beta_{1\text{-}42}$

$A\beta_{1\text{-}42}$ peptide was dissolved in sterilized double distilled water, prepared into a final concentration of 1 mM storage solution. Then, the solution was incubated in 37 °C for 7 days to prepare fibrillar $A\beta_{1\text{-}42}$ ($fA\beta_{1\text{-}42}$) and store in − 80 °C freezer for use (Xu et al. 2015). The aggregated states of $A\beta_{1\text{-}42}$ were checked by electron microscope. Briefly, $A\beta_{1\text{-}42}$ solution was absorbed onto a carbon-coated copper grid and then stained negatively with 1% phosphotungstic acid. After drying briefly, the samples were imaged with electron microscope (JEM-2100, JEOL, Japan) operating at 120 kV. The aged $A\beta_{1\text{-}42}$ mainly appeared fibrils although some other form of aggregates such as protofibrils also presented under electron microscope (Supplementary Fig. 1). In this text, the simplified fAβ was also used to represent fibrillar $A\beta_{1\text{-}42}$.

Stereotaxic Surgery

Adult wild-type C57BL/6J mice were randomly divided into two groups ($n = 4$ per group) and injected with 1 μl vehicle or fAβ (50 μM) into the unilateral hippocampus separately. Mice were anesthetized with sodium pentobarbital (45 mg/kg ip) and fixed to a stereotaxic instrument. A sagittal incision was made on the head. The intrahippocampal injection was performed with coordinates for the hippocampus: antero-posterior − 1.82 mm; lateral ± 1.13 mm respect to bregma, and depth of − 1.75 mm respect to the duramater, and with injecting at speed of 0.2 μl/min. After injection, the scalp was sutured and mice were put on a heating pad

for recovery. Then, the mice were sacrificed on the fourth day after surgery and brain slices (thickness 25 μm) were prepared for immunofluorescent staining.

Cell Culture and Treatment

BV2 cells were obtained from American Type Culture Collection (Manassas, VA) and cultured in Dulbecco's Modified Eagle's Medium (Gibco, USA) supplemented with 10% fetal bovine serum (Invitrogen, USA) and 1% antibiotic–antimycotic (Gibco, USA) in 37 °C, 5% CO_2 incubator. Cells were passaged every 2–3 days. For analyzing the effects of Aβ on BV2 migration, cells were transferred to the 3-well chamber as shown in Fig. 2a or the transwell system (Justus et al. 2014). For analyzing the Aβ-induced inflammation response of microglial BV2 cells, pretreatment of cells with LPS (100 ng/ml) for 6 h and washed with PBS. Then, cells were treated by fAβ (10 μM) with or without Fasudil (50 μM) and Y27632 (10 μM) for 24 h.

Cell Migration Assay

3-Well Chamber System

The slides were coated with PDL at 100 μg/ml in PBS overnight in 24-well plate. 3-Well chamber insert was set on the coated slides. As illustrated in Fig. 2a, 20 μl of fAβ (50 μM) or water was added into the side chambers and the chambers were air-dried overnight. BV2 cells were seeded in the middle chamber and incubated overnight for adherence (Fig. 2a). Then, the medium and the 3-well chamber insert were removed, followed with adding fresh medium. The chemotaxis effect of Aβ on BV2 cells was analyzed after 24 h.

For collecting enough cells to carry out the immunoblotting assay and RhoA activity assay, fAβ was added into all the three chambers, whereas BV2 cells were seeded in outer space of the chamber in 24-well plate (Fig. 3a). The insert was removed after cells adherence. Cells were harvested and subjected to immunoblotting analysis and RhoA activity assay after culturing for 24 h.

Transwell System

We used the 8.0 μm pore size culture insert (Corning Costar) in 24-well plates to assess the migration of BV2 cells. Cell suspension was added in the upper chamber of transwell system and fAβ (10 μM or 20 μM) was added into the lower chamber after cell adherence. To analyze the effect of Rho/ROCK signaling inhibitors on BV2 cell migration, Fasudil (50 μM) (Chen et al. 2017a) or Y27632 (10 μM) (Fu et al. 2016) was added into the upper chamber when adding fAβ. 24-h time period was given to allow cell migration. After that, cells on the membrane of the transwell insert were fixed with 4% paraformaldehyde. Cells that migrated to the undersurface of the membrane were stained with crystal violet. The experiments were repeated at least three times.

Cytotoxicity Assay

Cell viability of BV2 cells was measured by the CCK-8 assay and LDH release. BV2 cells were seeded in 96-well plates and incubated overnight. fAβ was added at the concentration of 1 μM, 5 μM, 10 μM and 20 μM, respectively, and treated for 24 h. For analyzing the protective effect of Rho/ROCK signaling inhibitors on Aβ-induced damage, cells were treated by fAβ (10 μM or 20 μM) with or without Fasudil (50 μM) and Y27632 (10 μM) for 24 h. The sequential CCK-8 assay and LDH release assay were performed according to the instructions. For morphological analysis, the phenotype of cluster formation in BV2 cells has been described (Huang et al. 2010). In this study, the cluster of more than 10 cells stacked upon each other was termed as the big cluster, and the cluster made by 5–10 cells was termed as the small cluster. The experiments were repeated at least three times.

Immunofluorescent Staining and Quantification

Samples (brain slices or cells) were fixed in 4% paraformaldehyde and washed three times with PBS. Then, samples were incubated in PBS with 10% horse serum and 0.2% Triton X-100 at 37 °C for 1 h. Next, samples were incubated with primary antibodies according to instructions for 1 h at 37 °C, and overnight at 4 °C. After three times wash in PBS, samples were incubated with secondary antibodies for 1 h at room temperature and followed with DAPI (10 μg/ml) incubation for 10 min. The immunofluorescence of cells was analyzed by Image J software (Schneider et al. 2012). Cells of interest were selected by the drawing tool of freehand. The parameters of "area integrated intensity" and "mean grey value" were selected to set the measurement. At least 30 cells were measured in each slide/region. To subtract the background, the density was calculated with the formula-integrated density − (area of selected cells × mean fluorescence of background readings). To analyze the distribution of CD16, CD206 and Thioflavin-S (Th-S) in amyloid plaques, the "Colocalization Finder" tool of Image J was used and the profiles were analyzed with a "Segmented Lines" tool with a line equals to 60 μm.

Western Blotting Analysis

BV2 cells were lysed with ice-cold RIPA buffer (50 mM Tris–HCl, 2 mM $MgCl_2$, 150 mM NaCl, 1% NP-40, 1 mM EDTA, 1 mM Na_3VO_4, 0.5 mM EGTA, and 0.25% sodium

deoxycholate) plus the cocktail of protease and phosphatase inhibitors for 30 min followed with centrifugation at 14,000 × *g* for 5 min at 4 °C. The supernatants were collected as protein samples and mixed with Laemmli buffer to denature. Equal amounts of proteins were separated by SDS–polyacrylamide gel and transferred to nitrocellulose membranes (Millipore, USA). The membranes were blocked in 5% nonfat milk in TBST (10 mM Tris–HCl, 150 mM NaCl, and 0.02% Tween-20, pH 7.5) and incubated overnight at 4 °C with the primary antibodies. Secondary antibodies were added according to the instructions. The immunoreactivity of protein bands was quantified using an Odyssey IR imaging system (LI-COR).

RhoA Pull-down Assay

RhoA pull-down assay was performed with the Rho Activation Assay Kit (Millipore, USA) to estimate the activated RhoA levels (Jo et al. 2002). The concentration of total protein in each sample was above 5 mg/ml. Briefly, cell lysate (500 µl) was combined with 20 µl Rhotekin RBD-agarose slurry and incubated at 4 °C with gentle agitation for 45 min. Rho regulates molecular events by cycling between an inactive GDP-bound form and an active GTP-bound form. In its active (GTP-bound) state, Rho could bind specifically to the Rho-binding domain (RBD) of Rhotekin. Then, the agarose beads were pelleted by brief centrifugation (10 s, 14,000 × *g*, 4 °C) and washed three times with 1 × Mg^{2+} lysis/wash buffer (MLB). The agarose beads were then resuspended in 25 µl of 2 × Laemmli buffer containing 4 µl dithiothreitol (DTT) and boiled for 5 min. The supernatant was collected, and the captured active RhoA was analyzed by western blot with anti-RhoA antibody.

Enzyme-Linked Immunosorbent Assay (ELISA) for IL-1 Detection

Pretreatment of BV2 cells with LPS (100 ng/ml) for 6 h and washed with PBS. Then, cells were treated by fAβ (10 µM) with or without Fasudil (50 µM) and Y27632 (10 µM). After 24 h, culture media were collected and centrifuged at 1000 × *g* for 10 min. The amounts of IL-1β in the culture medium were measured according to commercial ELISA kits instructions.

Statistical Analysis

Prism6.0 (GraphPad Software, San Diego, CA) was used for statistical analysis. All results were presented as mean ± SEM. The unpaired *t* test was used for comparisons between two groups. One-way ANOVA was used for comparisons across multiple groups. A value of $p < 0.05$ was statistically significant.

Results

Aβ Induces Microglial Activation Accompanied by Increase in RhoA Expression In Vivo

We first confirmed the pathological feature of reactive microglia concentrated around amyloid plaques. Microglial activation was analyzed by immunostaining of Iba-1 in brain sections of wild-type and APP/PS1 transgenic mice. As shown in Fig. 1a, there were few reactive microglia in the hippocampus of wild-type mice, but in APP/PS1 mice, microglia were highly activated and widely distributed throughout the entire hippocampus. Consistent with the previous findings, reactive microglia showed significant accumulation in Thioflavin-S (Th-S) labeled amyloid plaques.

Then, we examined the expression of RhoA in the brains of APP/PS1 mice. An interesting distribution pattern showed up that microglia in amyloid plaque-free (Th-S(−)) regions expressed the significant (relative) high level of RhoA than in amyloid plaque-enrich (Th-S(+)) regions (Fig. 1b, c).

We performed another in vivo test to inspect Aβ-induced microglia activation and RhoA expression. In the brains of wild-type mice, injecting with fAβ strongly induced the activation of microglia and the accumulation of microglia in the injected region, accompanied by the dramatic high expression of RhoA comparing those in vehicle-injected brains (Fig. 1d). Together, these results confirmed that Aβ is able to activate microglia and induces RhoA expression.

Aβ Induces Chemotactic Migration of BV2 Cells via RhoA/ROCK Signaling In Vitro

To probe the role of RhoA in Aβ-induced microglial chemotaxis, an in vitro cell migration assay was employed. As illustrated in Fig. 2a, the PDL coated slide was covered by a removable 3-well chamber insert. Wells on the two sides were plated with fAβ or vehicle accordingly, while the central one was seeded with BV2 cells, which are immortalized microglial cells being widely used. The model of chemotactic migration was established by removing the chamber and allowing BV2 cells to migrate through sensing the conditions on both sides. Therefore, a conditional environment containing the locally aggregated Aβ, which is for mimicking the existence of amyloid plaques in the brain, was constituted after removing the chamber insert. Cell migration was analyzed by comparing the number of cells between slide partitions. Through phase contrast imaging, we observed that Aβ attracted more BV2 cells migrated to its side and transition zone than vehicle (Fig. 2b), confirming the agonistic function of Aβ in microglial chemotaxis.

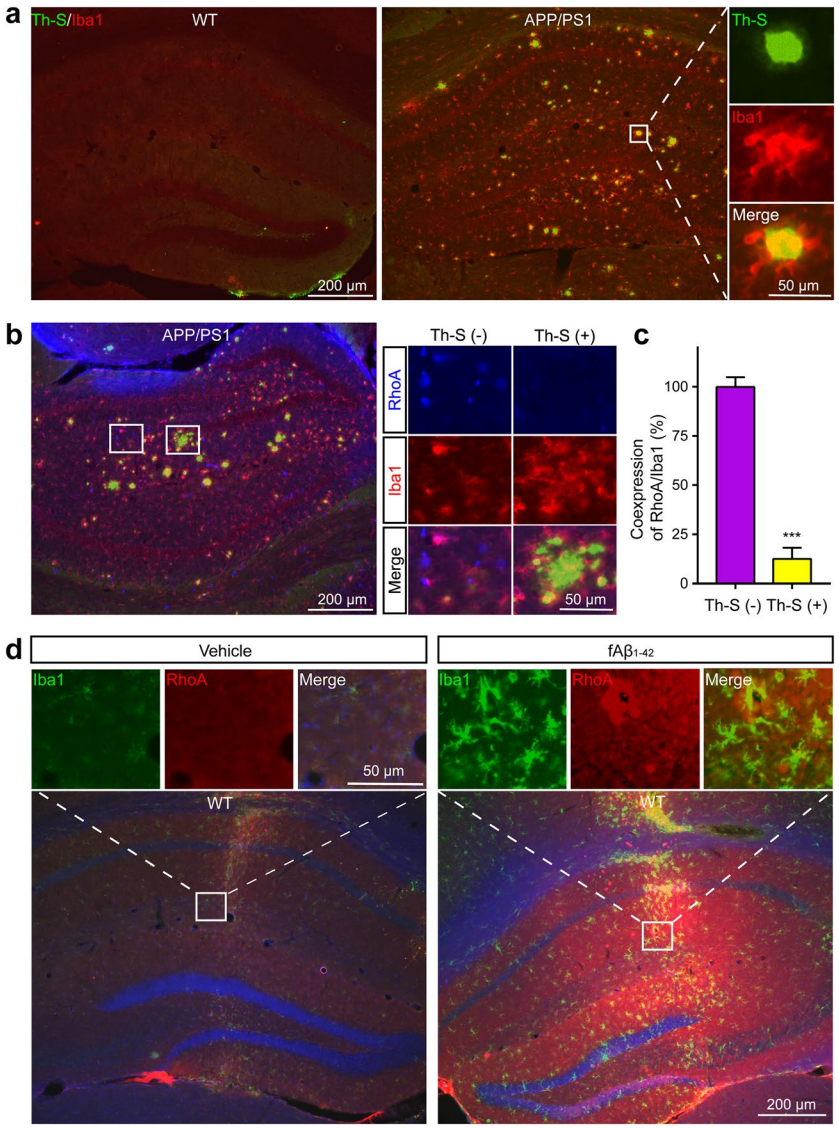

Fig. 1 Microglia activation and RhoA expression in vivo. **a** Distribution of Iba-1 (red) labeled reactive microglia in brains (hippocampus region) of wild-type and APP/PS1 transgenic mice. Amyloid plaques were stained by Th-S (green). **b** RhoA (blue) expression pattern in reactive microglia (Iba-1, red) in brains (hippocampus region) of APP/PS1 transgenic mice. Two representative regions, amyloid plaque free [Th-S(−)] and enriched [Th-S(+)], were magnified. **c** The coexpression of RhoA and Iba-1 in amyloid plaque free [Th-S(−)] and enriched [Th-S(+)] regions was quantified. **d** Iba-1 labeled microglial activation (green) and RhoA expression (red) in brains of vehicle or fAβ (50 μM) injected wild-type mice. All results were reported as mean ± SEM. ***$p < 0.001$

RhoA and its main effector ROCK were examined by immunostaining (Fig. 2c, d). Quantification of the fluorescence density showed that BV2 cells migrating to Aβ expressed significantly higher levels of RhoA and ROCK2 (the main isoform of ROCK in brain), coinciding with the occurrence of chemotactic response.

Filamentous actin (F-actin) is prominently regulated by RhoA/ROCK signaling to drive the morphological change and coordinate the migrating behavior of cells (Sit and Manser 2011). Therefore, we further detected F-actin with a high-affinity fluorescent probe and observed its upregulation in line with RhoA and ROCK2 (Fig. 2e). Notably, there was a significantly higher population of BV2 cells in the right transition zone (Aβ side) presented the structure of pseudopodium (Fig. 2e; Supplementary Fig. 2), which leads the way in cell migration (Chodniewicz and Klemke 2004), implying the activation of RhoA/ROCK signaling pathway.

Locally Aggregated Aβ Activates RhoA/ROCK Signaling in BV2 Cells

To explore whether Aβ activates RhoA/ROCK signaling, the 3-well chamber insert was applied in a different manner (Fig. 3a) to collect enough cells for biochemistry analysis. Instead of distinguishing the internal wells, we placed the chamber insert onto a plate for separating the inner (adding fAβ or vehicle) and outer (seeding BV2 cells) spaces. Immunoblotting of RhoA and ROCK2 revealed that locally aggregated Aβ did induce changes in their expression level. BV2 cells exposed to Aβ condition for 16 h showed an increasing trend of RhoA/ROCK2 (Fig. 3b, c), and when extended to 24 h, the increase reached a significant level (Fig. 3d, e).

RhoA acts as a binary switch by cycling between the active (GTP-bound) and inactive (GDP-bound) state. To obtain further insight into the activation of RhoA, we

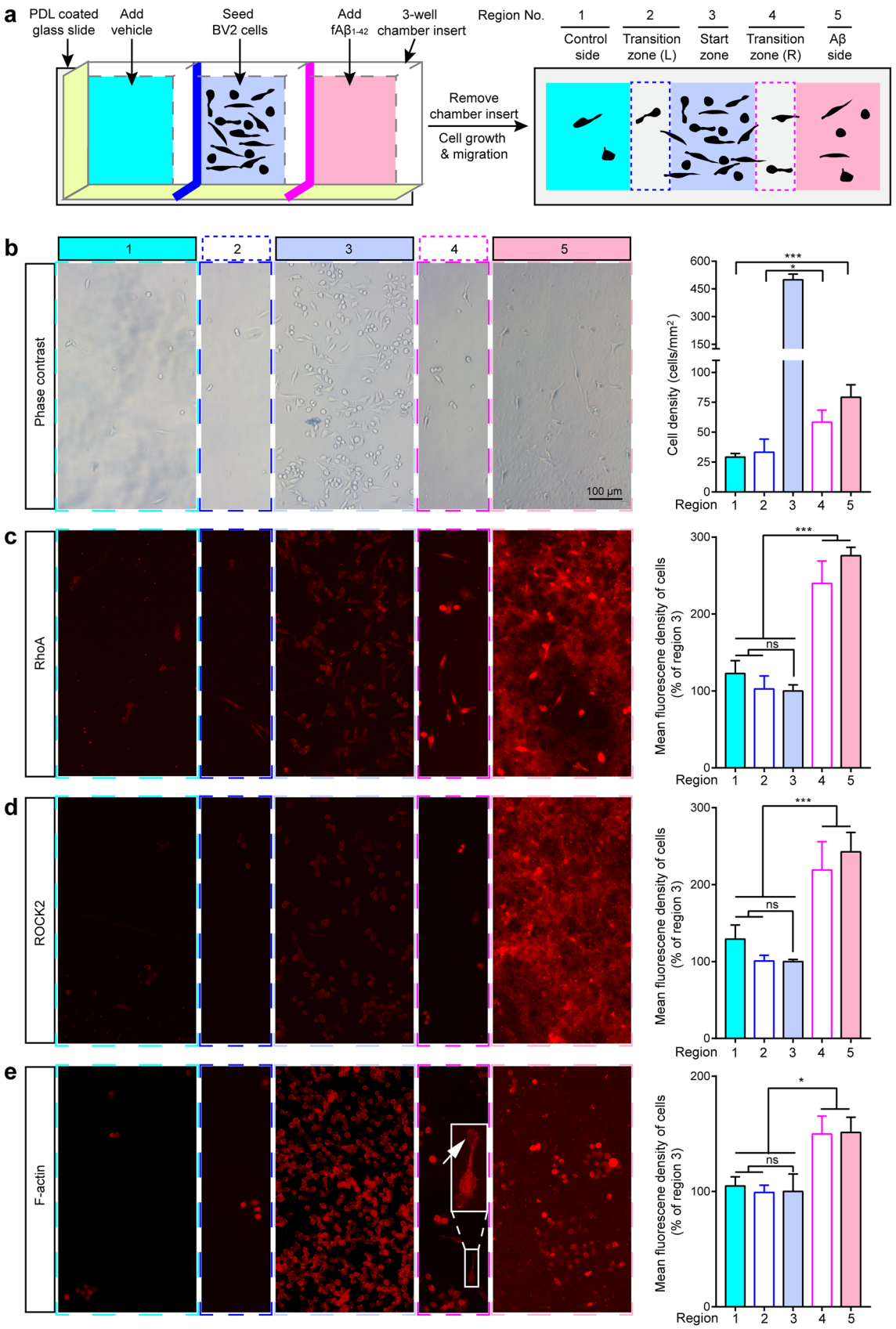
a
PDL coated glass slide
Add vehicle
Seed BV2 cells
Add fAβ1-42
3-well chamber insert
Region No.
1 Control side
2 Transition zone (L)
3 Start zone
4 Transition zone (R)
5 Aβ side
Remove chamber insert
Cell growth & migration
b
Phase contrast
100 μm
Cell density (cells/mm²)
Region
c
RhoA
Mean fluorescene density of cells (% of region 3)
ns
d
ROCK2
e
F-actin

◂**Fig. 2** Aβ-induced microglial chemotaxis and the involvement of RhoA/ROCK signaling. **a** Schematic diagram of the 3-well chamber-based cell migration system. **b** Aβ-induced chemotactic migration of BV2 cells was visualized by phase contrast imaging and the corresponding quantification. **c** and **d** Expression levels of RhoA and ROCK2 in different regions were detected by immunostaining and quantified by analyzing the mean fluorescence of cells. **e** F-actin expression and the formation of pseudopodium in BV2 cells were detected by fluorescent probe. Arrow in **e** indicates the structure of pseudopodium. All results were reported as mean ± SEM. *ns* No statistical significance, $*p < 0.05$, $***p < 0.001$

measured the GTP binding of RhoA by the pull-down assay. Clearly, a higher amount of GTP-RhoA was detected in cell lysate from Aβ condition (Fig. 3f) as well as an increase in total RhoA (Supplementary Fig. 3), demonstrating that aggregated Aβ could activate RhoA/ROCK signaling in BV2 cells.

Inhibiting RhoA/ROCK Signaling Suppresses Aβ-Induced Chemotaxis of BV2 Cells as well as Cytotoxicity

To determine whether RhoA/ROCK signaling is essential for Aβ-induced microglial chemotaxis, we introduced the classic transwell system for pharmacological manipulation. We first established the equilibrium of the system by filling both upper and lower compartments just with the medium. In this condition, only a small number of cells migrated to the undersurface (Fig. 4a). Then, we disrupted the equilibrium by having 10 or 20 μM fAβ in the lower compartment and found the massive migration of BV2 cells (Fig. 4a). We next antagonized RhoA/ROCK signaling by adding the widely used ROCK inhibitor Fasudil or Y27632 into the upper compartment (Fig. 4a). Treatment with Fasudil and Y27632 both significantly suppressed fAβ-induced cell migration (Fig. 4a–c), revealing the indispensability of RhoA/ROCK signaling. Although there appeared no significant difference in driving cell migration by fAβ with concentrations between 10 and 20 μM, with or without Fasudil, the suppression by Y27632 was much weaker when fAβ was at 20 μM (Fig. 4d). The possible reason was that Aβ-induced chemotaxis had reached the maximum level in this assay because the available paths for cell migration are limited. The application of Y27632 eliminated the saturation effect and exhibited the real trend that microglial chemotaxis depends on the load of Aβ, while Fasudil here dramatically suppressed microglial migration.

Through the transwell system, we were able to examine the characteristic of Aβ cytotoxicity in concentration gradient distribution. LDH release in up-chamber which was measured showed that the impaired cell viability was detected from the group of Aβ-induced chemotaxis. Again, we observed the remarkable inhibitory effect of Fasudil and Y27632 in this test (Fig. 4e), suggesting that RhoA/ROCK signaling is also associated with Aβ-induced cytotoxicity.

Protective Effect of RhoA/ROCK Signaling Inhibitors on Aβ-Induced Cytotoxicity and Inflammatory Response of BV2 cells

Microglia undergo direct interaction with Aβ in AD brain, so we switched to the cytotoxicity assays in which Aβ was added to BV2 cells directly. As expected, Aβ exhibited the dose-dependent toxicity on BV2 cells (Fig. 5a). Through two independent cell viability assays (CCK-8 assay and LDH release), we found the consistent phenomenon that Fasudil and Y27632 could significantly ameliorate the cytotoxicity induced by 10 μM Aβ but fail to do so for 20 μM Aβ (CCK-8 assay in Fig. 5b and LDH release assay in Supplementary Fig. 4a). We further checked the morphology of BV2 cells in different conditions. Treatment with 10 μM Aβ triggered the formation of cell clustering whereas with 20 μM Aβ led to relative severe cell damage. Correspondingly, Fasudil and Y27632 could drastically reduce the size of cell clusters induced by 10 μM Aβ (Fig. 5c; Supplementary Fig. 4b) but could not obviously rescue cellular atrophy induced by 20 μM Aβ (Supplementary Fig. 4b). Therefore, RhoA/ROCK signaling is involved in Aβ-induced microglial cytotoxicity.

RhoA/ROCK signaling inhibitors have been reported to show the promising effect in the treatment of neuroinflammation (Alokam et al. 2015; Chen et al. 2017b) in different models, but there is no clear evidence in the model of Aβ-induced microglial inflammatory response. Key players of the inflammatory cascade such as the inflammasome components NLRP3, CASP1 and the pro-inflammatory mediator IL-1β were analyzed. As shown in Fig. 5d, microglial BV2 cells were primed by LPS and further treated by Aβ in the presence/absence of ROCK inhibitors. The inflammasome complex proteins NLRP3 and pro-CASP1 were upregulated by Aβ treatment, and the ROCK inhibitors were able to suppress these effects (Fig. 5e). Consequently, the level of pro-IL1β, the production and release of pro-inflammatory mediator IL-1β were also showing similar changes (Fig. 5e–g). Taken together, these data confirmed the involvement of RhoA/ROCK signaling in Aβ-induced microglial inflammatory response.

Aβ-Induced Distribution Pattern of CD16 Positive and CD206 Positive Microglia

The dual function of microglial inflammatory response in AD model was assessed by analyzing the expression of pro-inflammatory marker CD16 and the anti-inflammatory marker CD206. In the chemotactic migration model in vitro, we observed the predominant upregulation of CD16 in BV2

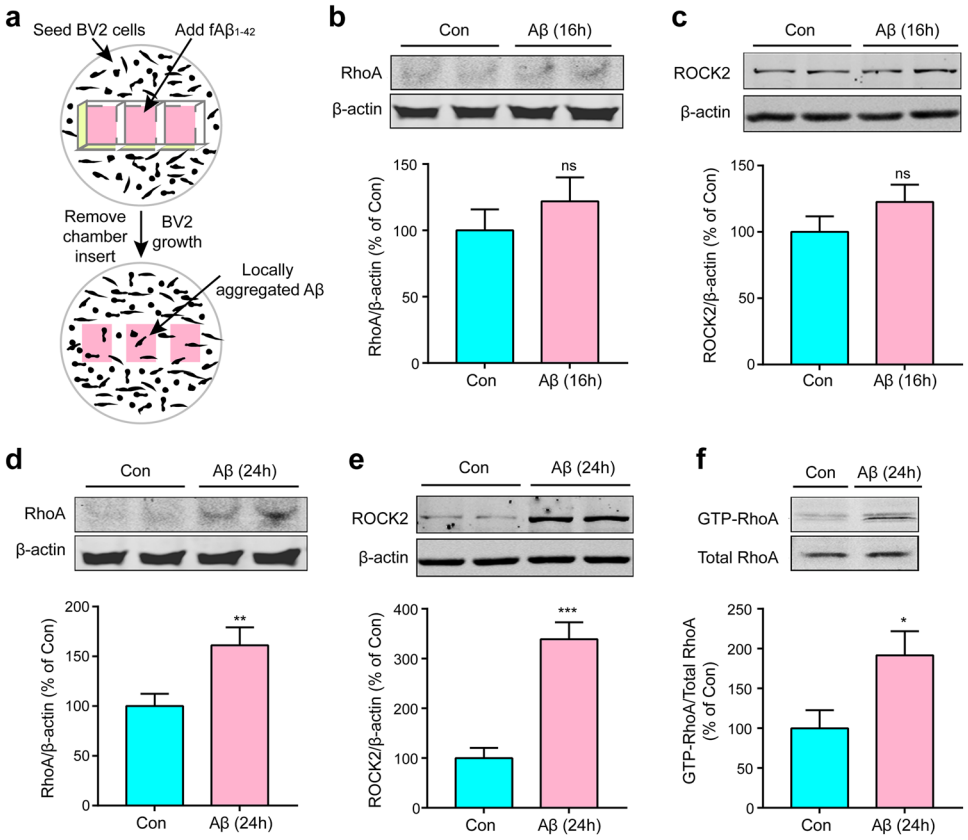

Fig. 3 Locally aggregated Aβ activates RhoA/ROCK signaling. **a** Schematic diagram of setting up the locally aggregated Aβ containing culture condition. **b**–**e** Western blot analysis of the upregulation of RhoA and ROCK2 induced by locally aggregated Aβ induces. **b** and **c** Increasing trend after 16 h Aβ treatment. **d** and **e** Significant elevation after 24 h Aβ treatment. **f** The GTP-RhoA was pulled down from the whole cell lysate and compared to the total RhoA. Locally aggregated Aβ significantly induced the GTP binding of RhoA. All results were reported as mean ± SEM. *ns* No statistical significance, $*p < 0.05$, $**p < 0.01$, $***p < 0.001$

cells from Aβ side (Fig. 6a–c), in accordance with the trend of RhoA/ROCK signaling (Fig. 2). However, when we turned to the in vivo model of APP/PS1 mice, we found a particularly interesting distribution pattern for CD16 and CD206. CD206 positive microglia were mainly enriched around amyloid plaques (Fig. 6d, e), whereas CD16 positive microglia were concentrated in amyloid plaques primarily (Fig. 6f, g). In addition, some microglia appeared to express both CD16 and CD206 (Fig. 6h, i, arrowhead) indicating the complex function of microglia in AD pathology. This phenomenon did not contradict to the observation from in vitro model, because microglial cells at Aβ plated side were localized in Aβ aggregates. Moreover, these results provided additional evidence for the beneficial effect of RhoA/ROCK signaling inhibitors in regulating neuroinflammation.

Discussion

Originally, when Alois Alzheimer first described the histopathology of AD, he also noted the abnormal morphology of glial cells (Alzheimer et al. 1995), which reflects the activation of glial cells. Nowadays, reactive microglia-mediated innate immune response is believed to plays an important role in AD pathogenesis (Solito and Sastre 2012). The prominent histopathological feature, reactive microglia surround amyloid plaques (Fig. 1a), has gained broad scientific interest. It has been evidenced that reactive microglia concentrated around amyloid plaques exhibit beneficial activity in Aβ clearance, but enigmatically, the much severe detrimental effect of neuroinflammation is also being triggered (Villegas-Llerena et al. 2016). Therefore, understanding the complex interplay between reactive microglia and amyloid plaque, especially Aβ, is extremely desirable.

Essential Role of RhoA/ROCK Signaling in Aβ-Induced Microglial Chemotaxis

The concept that Aβ function as a chemoattractant for microglia has been established (Davis et al. 1992) and several microglial cell surface players, such as chemokine ligands/receptors (El Khoury et al. 2007; Huang et al. 2010), chemoattractant receptor (Le et al. 2001) and Nogo receptor (Fang et al. 2018) have been discovered to regulate chemotaxis. However, the intracellular signaling pathway involved in this process is poorly understood. Here we presented that RhoA/ROCK signaling, the fundamental mediator of cell movement, regulates Aβ-induced microglial chemotactic migration. The cue was from in vivo mouse model, from the brains of both APP/PS1 transgenic mice and fAβ injected wild-type mice, we observed the high abundance of RhoA in reactive microglia which are mainly in amyloid-free regions

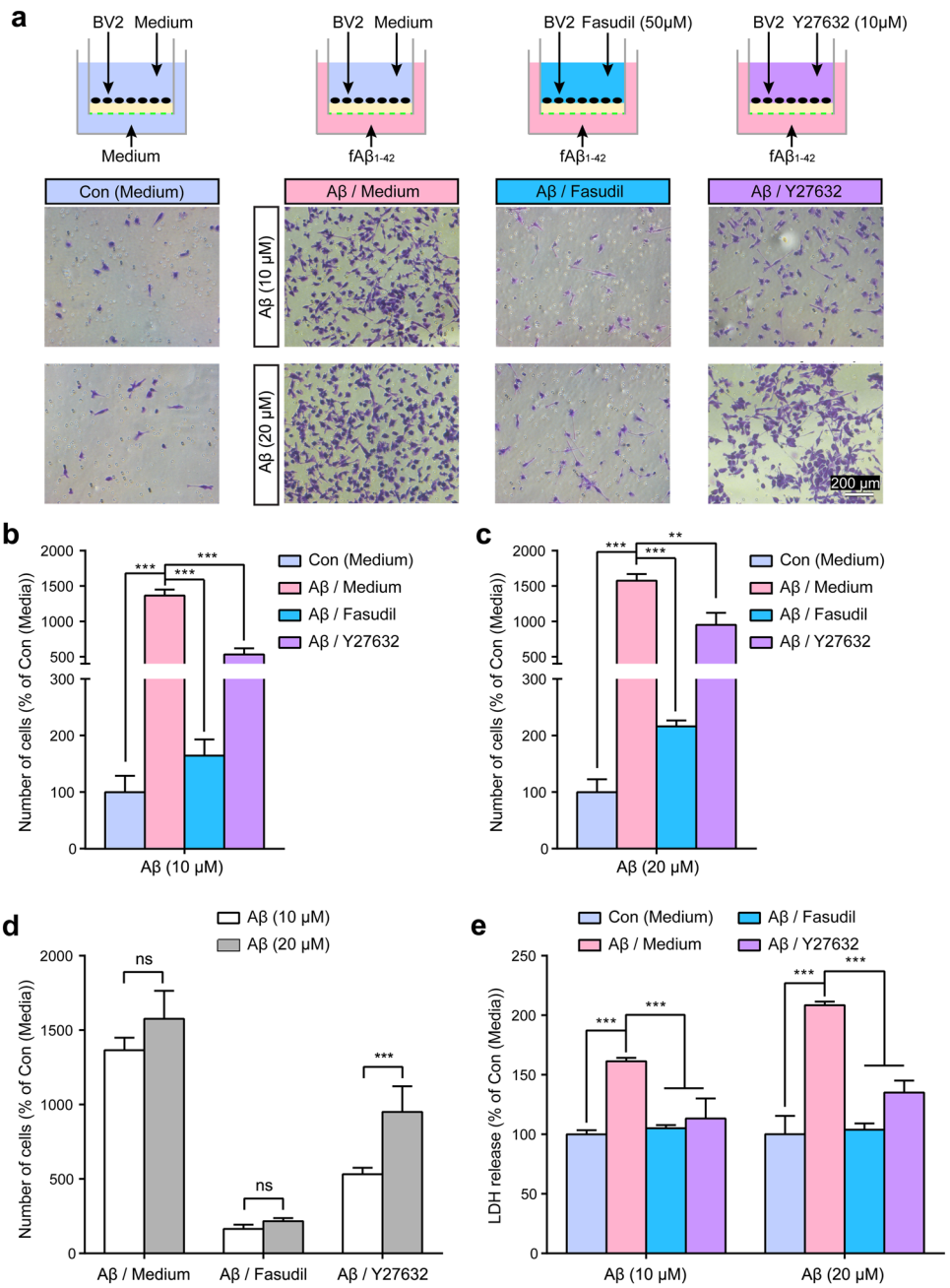

Fig. 4 Aβ-induced microglial chemotaxis was suppressed by inhibitors of RhoA/ROCK signaling. **a** Schematic diagram of transwell system conditions and the corresponding results of cell migration. Two concentrations of Aβ (10 and 20 μM) and two classical ROCK inhibitors (Fasudil 50 μM, Y27632 10 μM) were used. Cells were visualized by crystal violet (CV) staining and counted by Image J. **b** and **c** RhoA/ROCK signaling inhibitor Fasudil and Y27632 suppress Aβ-induced chemotaxis of BV2 cells. **b** Quantification of cell migration induced by 10 μM Aβ and the suppression effect of ROCK inhibitors. **c** Quantification of cell migration induced by 20 μM Aβ and the suppression effect of ROCK inhibitors. **d** Comparison of cell migration induced by 10 μM Aβ and 20 μM Aβ and the different suppression effects of Fasudil and Y27632. **e** LDH release in transwell assay was examined. Fasudil and Y27632 ameliorated Aβ-induced cytotoxicity of BV2 cells. All results were reported as mean ± SEM. *ns* No statistical significance, $^{**}p < 0.01$, $^{***}p < 0.001$

(Fig. 1b). Analysis of microglial chemotaxis based on the in vitro model provided direct evidence for the involvement of RhoA/ROCK signaling (Figs. 2, 3). The presence of F-actin labeled pseudopod morphology reinforced this idea because the universal effect of RhoA/ROCK on F-actin mediated cell movement has been well documented (Sit and Manser 2011) (Fig. 2e). Furthermore, the pharmacological manipulation of RhoA/ROCK signaling proved its indispensability in Aβ-induced microglial chemotaxis.

In this study, two classical inhibitors, Fasudil and Y27632, were tested and both showed prominent suppression effects Aβ-induced microglial chemotaxis. Notably, Fasudil appeared better efficiency than Y27632 when the higher amount of Aβ was applied (Fig. 4d). One reasonable explanation is the dose-dependent effect. The working doses of Fasudil (50 μM) and Y27632 (10 μM) in this study were based on previous studies which have shown their effectiveness (Fu et al. 2016; Chen et al. 2017b). Both Fasudil and Y27632 have been concerned as specific inhibitors for ROCK (Ishizaki et al. 2000), Ark et al. assessed the EC50 of Fasudil and Y27632 in vitro and found that these two inhibitors have very similar efficacy of regulation effects on smooth muscle contraction of human umbilical arteries (Ark et al. 2004), the mechanism

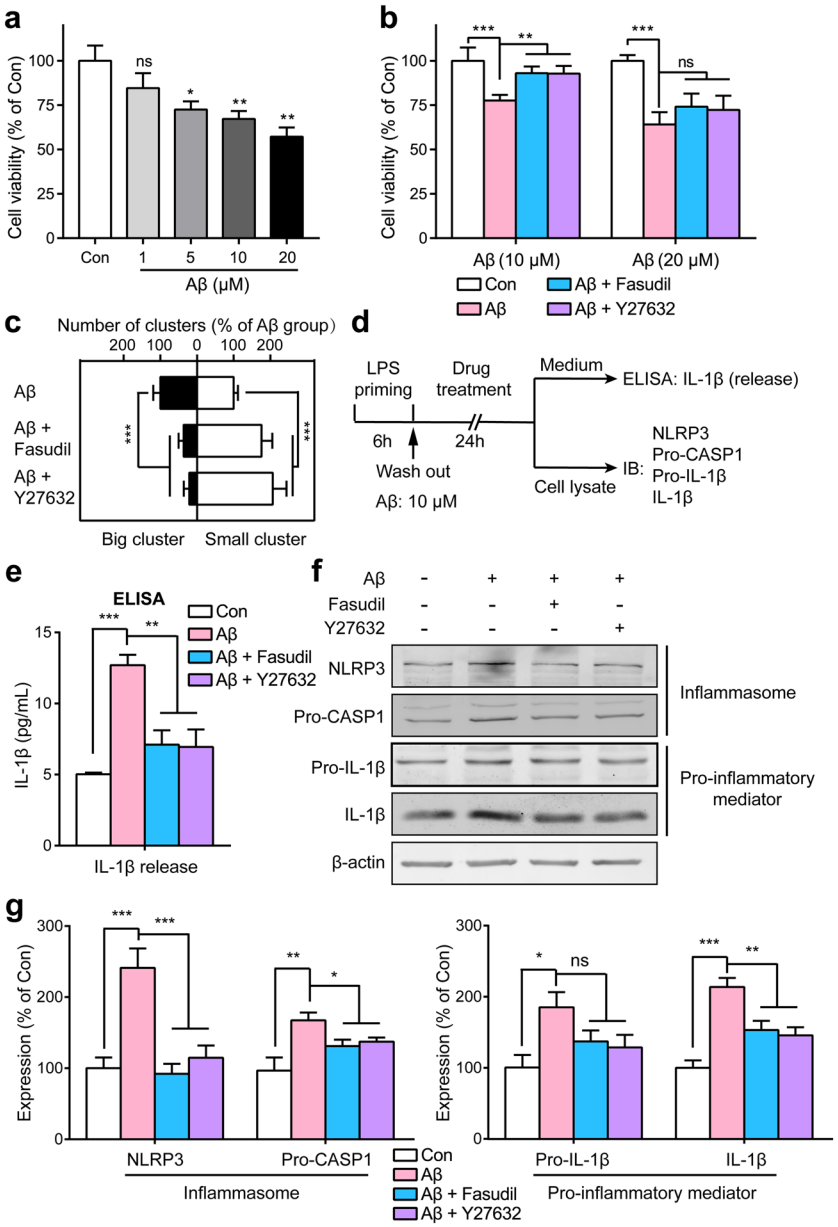

Fig. 5 RhoA/ROCK inhibitors suppressed Aβ-induced cytotoxicity and inflammatory response in BV2 cells. **a** Aβ-induced dose-dependent cytotoxicity in BV2 cells was detected by CCK-8 assay. **b** CCK-8 assay showed that Fasudil and Y27632 ameliorated Aβ-induced cytotoxicity of BV2 cells. **c** Aβ (10 μM)-induced microglial cell clustering was quantified. Big cluster means 10 or more cells aggregation, small cluster means 5–10 cells aggregation. Fasudil and Y27632 could inhibit cluster formation significantly. **d** Workflow of the inflammatory response detections. BV2 cells were primed by 100 ng/ml LPS for 6 h. LPS was washed out and the drug exposures (Con, 10 μM Aβ, 50 μM Fasudil and 10 μM Y27632) lasted for 24 h. Cells were lysed for western blot analysis, and the medium was assessed by ELISA for measuring IL-1β release. **e** Released IL-1β in culture medium was detected by ELISA. Fasudil and Y27632 strongly suppressed Aβ-induced IL-1β releasing. **f** Western blot analysis of inflammasome complex (NLRP3 and pro-CASP1) and pro-inflammatory mediator IL-1β. **g** The quantification analysis of the effects of Fasudil and Y27632 on Aβ-induced response of inflammasome complex-related elements. All results were reported as mean ± SEM. *ns* No statistical significance, $^{*}p < 0.05$, $^{**}p < 0.01$, $^{***}p < 0.001$

of which might be related to migration. In view of that, although we did not pursue the actual dose dependence, the better effect evoked by Fasudil (50 μM, higher dose) than Y27632 (10 μM, lower dose) is plausible to see.

In a recent finding of Aβ-induced microglial migration, Liao et al. also observed the activation of RhoA, which is consistent with our results. Interestingly, they also observed that microglial migration was inhibited even when RhoA activation was further enhanced by Nogo application. This seemingly confounding phenomenon could be due to other signaling pathways activation such as Rac1 and CDC42. The detailed mechanism needs further investigation (Fang et al. 2018).

Beneficial Effect of Anti-RhoA/ROCK Signaling in Aβ-Induced Microglial Cytotoxicity and Inflammatory Response

The hypothesis of microglia dysfunction in AD pathogenesis has emerged (Mosher and Wyss-Coray 2014), which indicates the importance of microglia in the healthy state. In the context of AD, the cytotoxic effect of Aβ is known to alter microglial activity and promote the release of cytokines (Small et al. 2001), which are the mediators of neuroinflammation. In this study, increased LDH release was detected even in the scenario of indirect interaction between Aβ and microglial cells (transwell assay, Fig. 4e). Direct exposure

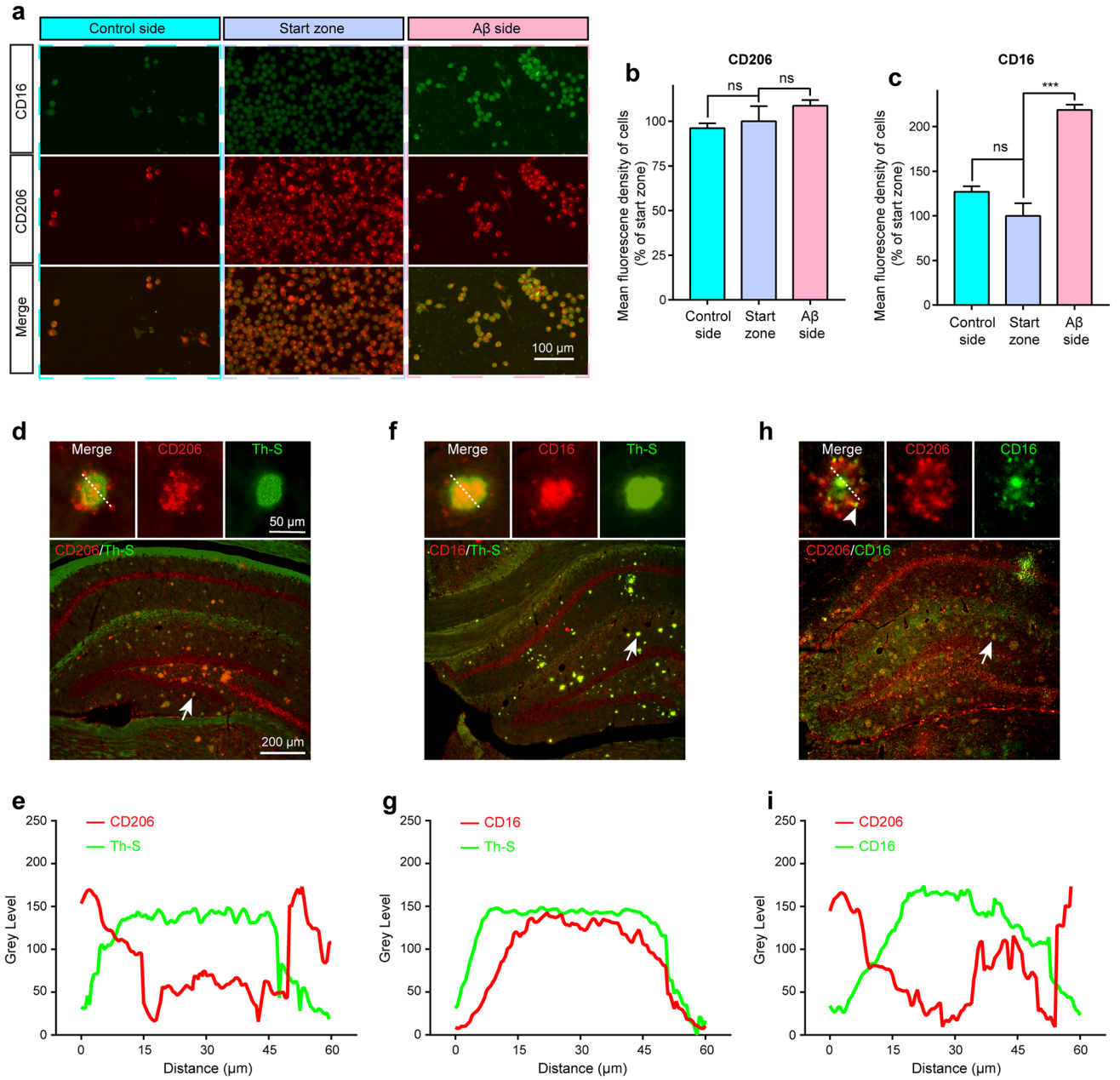

Fig. 6 Distribution pattern of CD16 positive and CD206 positive microglia. **a** Upregulation of CD16 (green) but not CD206 (red) in BV2 cells that migrated to Aβ aggregates. **b** and **c** Quantification of immunofluorescence density of CD206 (**b**) and CD16 (**c**) in BV2 cells. **d** and **e** CD206 immunopositive signals (red) are tended to be enriched around Th-S (green) labeled amyloid plaques in hippocampus of APP/PS1 mice. The dash line indicates the actual segment for measuring the distribution of gray levels of red and green signals in a representative plaque. **f** and **g** CD16 immunopositive signals (red) are tended to be concentrated in Th-S (green) labeled amyloid plaques. The dash line indicates the actual segment for measuring the distribution of gray levels of red and green signals in a representative plaque. **h** and **i** Amyloid plaques recruited microglia can express CD16 (green) and CD206 (red) simultaneously with differential distribution. The dash line indicates the actual segment for measuring the distribution of gray levels of red and green signals in a representative plaque. Arrow ahead indicates coexpression of CD16 and CD206. All results were reported as mean ± SEM. *ns* No statistical significance, $***p < 0.001$

to Aβ triggered not only the decrease in cell viability but also the formation of cell cluster, a microglial phenomenon which might indicate the immune activation (Fig. 5c) (van Horssen et al. 2012).

The assessment of NLRP3-inflammasome and the pro-inflammatory mediator IL-1β confirmed that Aβ is able to induce the inflammatory response of microglial cells, which is consistent with the previous reports (Small

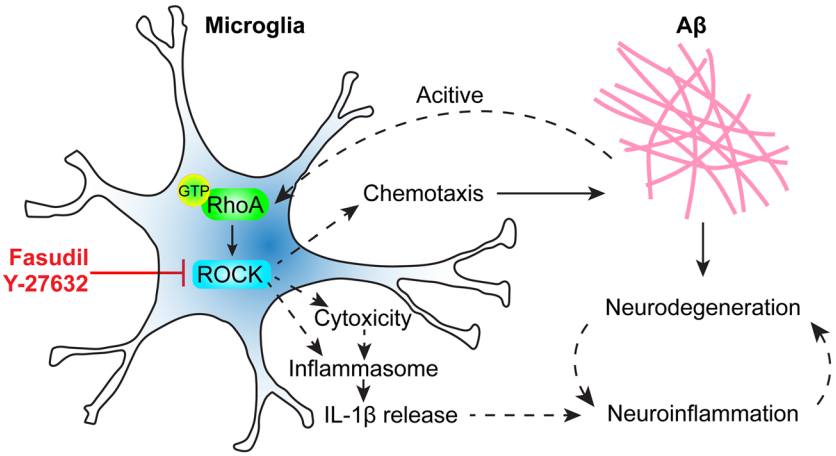

Fig. 7 Proposed model for the role of RhoA/ROCK signaling in Aβ-induced microglial response and the potential consequence

et al. 2001). Fasudil and Y27632 could efficiently suppress these inflammatory responses (Fig. 5), implying that anti-RhoA/ROCK signaling pathway is beneficial for microglia dysfunction. Indeed, interfering with RhoA/ROCK signaling has shown the promising effect in AD research, such as reducing the level of Aβ and stimulating the regenerative growth of neurites (Mueller et al. 2005). Our finding provided additional evidence to support the therapeutic potential of RhoA/ROCK signaling inhibitors in AD treatment.

RhoA/ROCK Signaling Involves in Microglia Mediates Neuroinflammation

The general model for distinguishing two types of microglial activation states, namely the pro-inflammatory M1 state and the anti-inflammatory M2 state, has been recently questioned (Ransohoff 2016). We also observed the co-expression of the so-called pro-inflammatory marker CD16 and anti-inflammatory marker CD206 (Chen et al. 2017a) from in vitro and in vivo models (Fig. 6f). Interestingly, the elevated levels of RhoA/ROCK (Fig. 2) and CD16 (Fig. 6a) were detected from microglial BV2 cells located in Aβ aggregates in vitro. The consistent trend might imply a possible link between RhoA/ROCK signaling and neuroinflammation. RhoA has been reported to modulate Aβ caused superoxide production in BV2 cells. Sequentially, the production of superoxide may lead to cytokine release and inflammatory response (Moon et al. 2013). Our results also provided the direct evidence of Aβ-induced microglial inflammatory response of which RhoA/ROCK signaling was involved (Fig. 5) as indicated by previous reports showing the suppression effect of RhoA/ROCK signaling on neuroinflammation in other models (Chen et al. 2017a, b; Alokam et al. 2015).

Conclusion

Taken together, we postulated the hypothesis that activation of RhoA/ROCK signaling induced by Aβ is involved in microglial chemotactic migration, cytotoxicity and inflammatory response. The accumulated microglia are dysfunctional and provoke the inflammatory response, thus leading to the vicious cycle of neuroinflammation and neurodegeneration. RhoA/ROCK signaling inhibitors are potential therapeutic agents for AD treatment (Fig. 7).

Acknowledgements This work was supported by the National Natural Science Foundation of China, Grant Numbers 31671041 and 81471285.

Author Contributions X.Z. performed all the experiments and wrote the manuscript. P.Y. contributed to part of immunofluorescence staining, cell culture and data analysis. D.W. contributed to write and review the manuscript. Y.W., L.C. and Y.L. contributed to some of in vitro analysis. C.Z. and Y.X. designed the study, analyzed data, and wrote the manuscript. All authors reviewed and approved the final manuscript.

Data Availability The datasets generated during and/or analyzed during the current study are available from the corresponding author on a reasonable request.

Compliance with Ethical Standards

Conflict of interest The authors declare that they have no conflict of interest.

Ethics Approval All applicable international, national, and/or institutional guidelines for the care and use of animals were followed. This article does not contain any studies with human participants performed by any of the authors.

References

Alokam R, Singhal S, Srivathsav GS, Garigipati S, Puppala S, Sriram D, Perumal Y (2015) Design of dual inhibitors of ROCK-I and NOX2 as potential leads for the treatment of neuroinflammation associated with various neurological diseases including autism spectrum disorder. Mol Biosyst 11(2):607–617. https://doi.org/10.1039/c4mb00570h

Alzheimer A, Stelzmann RA, Schnitzlein HN, Murtagh FR (1995) An English translation of Alzheimer's 1907 paper, "Uber eine eigenartige Erkankung der Hirnrinde". Clin Anat 8(6):429–431. https://doi.org/10.1002/ca.980080612

Ark M, Ozveren E, Yazici G, Korkmaz B, Buyukafsar K, Arikan O, Kubat H, Songu-Mize E (2004) Effects of HA-1077 and Y-27632, two rho-kinase inhibitors, in the human umbilical artery. Cell Biochem Biophys 41(3):331–342. https://doi.org/10.1385/CBB:41:3:331

Chen TJ, Hung HS, Wang DC, Chen SS (2010) The protective effect of Rho-associated kinase inhibitor on aluminum-induced neurotoxicity in rat cortical neurons. Toxicol Sci 116(1):264–272. https://doi.org/10.1093/toxsci/kfq114

Chen J, Sun Z, Jin M, Tu Y, Wang S, Yang X, Chen Q, Zhang X, Han Y, Pi R (2017a) Inhibition of AGEs/RAGE/Rho/ROCK pathway suppresses non-specific neuroinflammation by regulating BV2 microglial M1/M2 polarization through the NF-kappaB pathway. J Neuroimmunol 305:108–114. https://doi.org/10.1016/j.jneuroim.2017.02.010

Chen J, Yin W, Tu Y, Wang S, Yang X, Chen Q, Zhang X, Han Y, Pi R (2017b) L-F001, a novel multifunctional ROCK inhibitor, suppresses neuroinflammation in vitro and in vivo: Involvement of NF-kappaB inhibition and Nrf2 pathway activation. Eur J Pharmacol 806:1–9. https://doi.org/10.1016/j.ejphar.2017.03.025

Chodniewicz D, Klemke RL (2004) Guiding cell migration through directed extension and stabilization of pseudopodia. Exp Cell Res 301(1):31–37. https://doi.org/10.1016/j.yexcr.2004.08.006

Davis JB, McMurray HF, Schubert D (1992) The amyloid beta-protein of Alzheimer's disease is chemotactic for mononuclear phagocytes. Biochem Biophys Res Commun 189(2):1096–1100

Ebrahimi T, Rust M, Kaiser SN, Slowik A, Beyer C, Koczulla AR, Schulz JB, Habib P, Bach JP (2018) Alpha1-antitrypsin mitigates NLRP3-inflammasome activation in amyloid beta1-42-stimulated murine astrocytes. J Neuroinflamm 15(1):282. https://doi.org/10.1186/s12974-018-1319-x

El Khoury J, Toft M, Hickman SE, Means TK, Terada K, Geula C, Luster AD (2007) Ccr2 deficiency impairs microglial accumulation and accelerates progression of Alzheimer-like disease. Nat Med 13(4):432–438. https://doi.org/10.1038/nm1555

Fan Y, Xie L, Chung CY (2017) Signaling pathways controlling microglia chemotaxis. Mol Cells 40(3):163–168. https://doi.org/10.14348/molcells.2017.0011

Fang Y, Wang J, Yao L, Li C, Wang J, Liu Y, Tao X, Sun H, Liao H (2018) The adhesion and migration of microglia to beta-amyloid (Abeta) is decreased with aging and inhibited by Nogo/NgR pathway. J Neuroinflamm 15(1):210. https://doi.org/10.1186/s12974-018-1250-1

Fu P, Tang R, Yu Z, Li C, Chen X, Xie M, Wang W, Luo X (2016) Rho-associated kinase inhibitors promote microglial uptake via the ERK signaling pathway. Neurosci Bull 32(1):83–91. https://doi.org/10.1007/s12264-016-0013-1

Fu W, Vukojevic V, Patel A, Soudy R, MacTavish D, Westaway D, Kaur K, Goncharuk V, Jhamandas J (2017) Role of microglial amylin receptors in mediating beta amyloid (Abeta)-induced inflammation. J Neuroinflamm 14(1):199. https://doi.org/10.1186/s12974-017-0972-9

Holtzman DM, Morris JC, Goate AM (2011) Alzheimer's disease: the challenge of the second century. Sci Transl Med 3(77):77sr71. https://doi.org/10.1126/scitranslmed.3002369

Huang WC, Yen FC, Shie FS, Pan CM, Shiao YJ, Yang CN, Huang FL, Sung YJ, Tsay HJ (2010) TGF-beta1 blockade of microglial chemotaxis toward Abeta aggregates involves SMAD signaling and down-regulation of CCL5. J Neuroinflamm 7:28. https://doi.org/10.1186/1742-2094-7-28

Ishizaki T, Uehata M, Tamechika I, Keel J, Nonomura K, Maekawa M, Narumiya S (2000) Pharmacological properties of Y-27632, a specific inhibitor of rho-associated kinases. Mol Pharmacol 57(5):976–983

Jeon YJ, Won HY, Moon MY, Choi WH, Chang CH, Lee JY, Kim J, Kim SC, Kim YS, Park JB (2008) Interaction of microglia and amyloid-beta through beta2-integrin is regulated by RhoA. Neuroreport 19(17):1661–1665. https://doi.org/10.1097/WNR.0b013e3283140f10

Jo M, Thomas KS, Somlyo AV, Somlyo AP, Gonias SL (2002) Cooperativity between the Ras-ERK and Rho-Rho kinase pathways in urokinase-type plasminogen activator-stimulated cell migration. J Biol Chem 277(14):12479–12485. https://doi.org/10.1074/jbc.M111147200

Justus CR, Leffler N, Ruiz-Echevarria M, Yang LV (2014) In vitro cell migration and invasion assays. J Vis Exp. https://doi.org/10.3791/51046

Le Y, Gong W, Tiffany HL, Tumanov A, Nedospasov S, Shen W, Dunlop NM, Gao JL, Murphy PM, Oppenheim JJ, Wang JM (2001) Amyloid (beta)42 activates a G-protein-coupled chemoattractant receptor, FPR-like-1. J Neurosci 21(2):RC123

Meraz-Rios MA, Toral-Rios D, Franco-Bocanegra D, Villeda-Hernandez J, Campos-Pena V (2013) Inflammatory process in Alzheimer's disease. Front Integr Neurosci 7:59. https://doi.org/10.3389/fnint.2013.00059

Moon MY, Kim HJ, Li Y, Kim JG, Jeon YJ, Won HY, Kim JS, Kwon HY, Choi IG, Ro E, Joe EH, Choe M, Kwon HJ, Kim HC, Kim YS, Park JB (2013) Involvement of small GTPase RhoA in the regulation of superoxide production in BV2 cells in response to fibrillar Abeta peptides. Cell Signal 25(9):1861–1869. https://doi.org/10.1016/j.cellsig.2013.05.023

Mosher KI, Wyss-Coray T (2014) Microglial dysfunction in brain aging and Alzheimer's disease. Biochem Pharmacol 88(4):594–604. https://doi.org/10.1016/j.bcp.2014.01.008

Mueller BK, Mack H, Teusch N (2005) Rho kinase, a promising drug target for neurological disorders. Nat Rev Drug Discov 4(5):387–398. https://doi.org/10.1038/nrd1719

Park JC, Baik SH, Han SH, Cho HJ, Choi H, Kim HJ, Choi H, Lee W, Kim DK, Mook-Jung I (2017) Annexin A1 restores Abeta1-42 -induced blood–brain barrier disruption through the inhibition of RhoA-ROCK signaling pathway. Aging Cell 16(1):149–161. https://doi.org/10.1111/acel.12530

Raftopoulou M, Hall A (2004) Cell migration: Rho GTPases lead the way. Dev Biol 265(1):23–32

Ransohoff RM (2016) A polarizing question: do M1 and M2 microglia exist? Nat Neurosci 19(8):987–991. https://doi.org/10.1038/nn.4338

Scheiblich H, Bicker G (2017) Regulation of microglial phagocytosis by RhoA/ROCK-inhibiting drugs. Cell Mol Neurobiol 37(3):461–473. https://doi.org/10.1007/s10571-016-0379-7

Schneider CA, Rasband WS, Eliceiri KW (2012) NIH Image to ImageJ: 25 years of image analysis. Nat Methods 9(7):671–675

Selkoe DJ, Hardy J (2016) The amyloid hypothesis of Alzheimer's disease at 25 years. EMBO Mol Med 8(6):595–608. https://doi.org/10.15252/emmm.201606210

Sellers KJ, Elliott C, Jackson J, Ghosh A, Ribe E, Rojo AI, Jarosz-Griffiths HH, Watson IA, Xia W, Semenov M, Morin P, Hooper NM, Porter R, Preston J, Al-Shawi R, Baillie G, Lovestone S,

Cuadrado A, Harte M, Simons P, Srivastava DP, Killick R (2018) Amyloid beta synaptotoxicity is Wnt-PCP dependent and blocked by Fasudil. Alzheimers Dement 14(3):306–317. https://doi.org/10.1016/j.jalz.2017.09.008

Sheng JG, Mrak RE, Griffin WS (1997) Neuritic plaque evolution in Alzheimer's disease is accompanied by transition of activated microglia from primed to enlarged to phagocytic forms. Acta Neuropathol 94(1):1–5

Sindi S, Mangialasche F, Kivipelto M (2015) Advances in the prevention of Alzheimer's disease. F1000Prime Rep 7:50. https://doi.org/10.12703/P7-50

Sit ST, Manser E (2011) Rho GTPases and their role in organizing the actin cytoskeleton. J Cell Sci 124(Pt 5):679–683. https://doi.org/10.1242/jcs.064964

Small DH, Mok SS, Bornstein JC (2001) Alzheimer's disease and Abeta toxicity: from top to bottom. Nat Rev Neurosci 2(8):595–598. https://doi.org/10.1038/35086072

Solito E, Sastre M (2012) Microglia function in Alzheimer's disease. Front Pharmacol 3:14. https://doi.org/10.3389/fphar.2012.00014

Tsushima H, Emanuele M, Polenghi A, Esposito A, Vassalli M, Barberis A, Difato F, Chieregatti E (2015) HDAC6 and RhoA are novel players in Abeta-driven disruption of neuronal polarity. Nat Commun 6:7781. https://doi.org/10.1038/ncomms8781

van Horssen J, Singh S, van der Pol S, Kipp M, Lim JL, Peferoen L, Gerritsen W, Kooi EJ, Witte ME, Geurts JJ, de Vries HE, Peferoen-Baert R, van den Elsen PJ, van der Valk P, Amor S (2012) Clusters of activated microglia in normal-appearing white matter show signs of innate immune activation. J Neuroinflamm 9:156. https://doi.org/10.1186/1742-2094-9-156

Venneti S, Wiley CA, Kofler J (2009) Imaging microglial activation during neuroinflammation and Alzheimer's disease. J Neuroimmune Pharmacol 4(2):227–243. https://doi.org/10.1007/s11481-008-9142-2

Villegas-Llerena C, Phillips A, Garcia-Reitboeck P, Hardy J, Pocock JM (2016) Microglial genes regulating neuroinflammation in the progression of Alzheimer's disease. Curr Opin Neurobiol 36:74–81. https://doi.org/10.1016/j.conb.2015.10.004

Wolf SA, Boddeke HW, Kettenmann H (2017) Microglia in physiology and disease. Annu Rev Physiol 79:619–643. https://doi.org/10.1146/annurev-physiol-022516-034406

Xu Y, Wang D, Luo Y, Li W, Shan Y, Tan X, Zhu C (2015) Beta amyloid-induced upregulation of death receptor 6 accelerates the toxic effect of N-terminal fragment of amyloid precursor protein. Neurobiol Aging 36(1):157–168. https://doi.org/10.1016/j.neurobiolaging.2014.07.027